Proceedings of the ASME 2017 Conference on Smart Materials, Adaptive Structures and Intelligent Systems
SMASIS2017
September 18-20, 2017, Snowbird, UT, USA

SMASIS2017-3820

SYNAPSE-INSPIRED VARIABLE CONDUCTANCE IN BIOMEMBRANES: A PRELIMINARY STUDY

Joseph S. Najem
Joint Institute for Biological Sciences, University of Tennessee - Oak Ridge National Laboratory
Oak Ridge, TN 37830, USA

Graham J. Taylor
Bredesen Center for Interdisciplinary Research, University of Tennessee - Oak Ridge National Laboratory
Oak Ridge, TN 37830, USA

Charles P. Collier
Center for Nanophase Materials Sciences, Oak Ridge National Laboratory[1]
Oak Ridge, TN 37830, USA

Stephen A. Sarles
Department of Mechanical, Aerospace and Biomedical Engineering, University of Tennessee, Knoxville, TN 37916, USA

ABSTRACT

Memristors are solid-state devices that exhibit voltage-controlled conductance. This tunable functionality enables the implementation of biologically-inspired synaptic functions in solid-state neuromorphic computing systems. However, while memristors are meant to emulate an intricate signal transduction process performed by soft biomolecular structures, they are commonly constructed from silicon- or polymer-based materials. As a result, the volatility, intricate design, and high-energy resistance switching in memristive devices, usually, leads to energy consumption in memristors that is several orders of magnitude higher than in natural synapses. Additionally, solid-state memristors fail to achieve the coupled dynamics and selectivity of synaptic ion exchange that are believed to be necessary for initiating both short- and long-term potentiation (STP and LTP) in neural synapses, as well as paired-pulse facilitation (PPF) in the presynaptic terminal. LTP is a phenomenon mostly responsible for driving synaptic learning and memory, features that enable signal transduction between neurons to be history-dependent and adaptable. In contrast, current memristive devices rely on engineered external programming parameters to imitate LTP. Because of these fundamental differences, we believe a biomolecular approach offers untapped potential for constructing synapse-like systems. Here, we report on a synthetic biomembrane system with biomolecule-regulated (alamethicin) variable ion conductance that emulates vital operational principals of biological synapse. The proposed system consists of a synthetic droplet interface bilayer (DIB) assembled at the conjoining interface of two monolayer-encased aqueous droplets in oil. The droplets contain voltage-activated alamethicin (Alm) peptides, capable of creating conductive pathways for ion transport through the impermeable lipid membrane. The insertion of the peptides and formation of transmembrane ion channels is achieved at externally applied potentials higher than ~70 mV. Just like in biological synapses, where the incorporation of additional receptors is responsible for changing the synaptic weight (i.e. conductance), we demonstrate that the weight of our synaptic mimic may be changed by controlling the number of alamethicin ion channels created in a synthetic lipid membrane. More alamethicin peptides are incorporated by increasing the post-threshold external potential, thus leading to higher conductance levels for ion transport. The current-voltage responses of the alamethicin-based synapse also exhibit significant “pinched”

[1] Notice: This manuscript has been authored by UT-Battelle, LLC, under Contract No. DE-AC0500OR22725 with the U.S. Department of Energy. The United States Government retains and the publisher, by accepting the article for publication, acknowledges that the United States Government retains a non-exclusive, paid-up, irrevocable, world-wide license to publish or reproduce the published form of this manuscript, or allow others to do so, for the United States Government purposes.

hysteresis—a characteristic of memristors that is fundamental to mimicking synapse plasticity. We demonstrate the system's capability of exhibiting STP/PPF behaviors in response to high-frequency 50 ms, 150 mV voltage pulses. We also present and discuss an analytical model for an alamethicin-based memristor, classifying that later as a "generic memristor".

INTRODUCTION

Neuromoprhic computing usually refers to sophisticated, solid-state electronic circuitries that emulate neuro-biological architectures found in the nervous system [1]. These circuitries have traditionally relied on analog or software-controlled very-large-scale integration (VLSI) models [2], or neuromorphic hardware such as memristors [3], and transistors [4], to perform brain-like computational operations. Memristors, in specific, have become ubiquitous in neuromorphic systems due to their ability to exhibit voltage-controlled conductance [3]. In its simplest form, a memristor (a concatenation of "memory resistor") is best described as a two-terminal device that is capable of adaptively regulating the flow of electrical current in a circuit as a function of voltage [5]. Unlike a resistor, the resistance in a memristor (i.e. memristance) is variable, and thus, it exhibits a "figure 8" shaped or "pinched" hysteresis loop in the voltage-current plane in response to a periodic voltage input, as opposed to a linear non-hysteric response in the case of a resistor [5]. Memristors are considered to be subsets of a more general class of memristive devices and could generally be classified into three families identified as Ideal Memristors, Generic Memristors, and Extended Memristors [6]. The existence of memristors as a concept dates back the 1971 when Leon Chua hypothesized, in a famous study [7], that a fourth circuit element (i.e. the memristor) is missing. However, and despite multiple experimental attempts (a couple examples are [8] and [9]), it was not until 2008 that the first commercial and physical memristor was realized by HP [10]. That first memristor consisted a thin-film of insulating titanium oxide (TiO_2) sandwiched between two platinum (Pt) layers. Ever since the metal/oxide/metal type memristors dominated the neuromorphic scene. Various two-terminal and three-terminal, metal-oxide memristors have been heavily employed to emulate synaptic dynamics [11]. The switching behavior (i.e. conductance change) in these devices is based on a thin-film Metal-Insulator-Metal (MIM), where the insulator layer is composed of one or more metal oxides with semiconducting properties [11]. These devices usually exhibit a range of internal resistive states, which are tunable in a quasi-stable manner. However, while they do bear limited similarity to biological synapses at the mechanism level, they fail to mimic the basic transport properties of biological neural networks. As a result, solid-state/silicon-based systems require far more power to achieve computational capabilities similar to biological systems. In an effort to close the gap between the MIM-based memristors and actual biological synaptic processes, multiple types of ionic-drift-based memristors (drift-type) have been designed and built [12-14]. However, even though drift-type memristors are a step closer to natural processes, they remain very far from exact replication of their biocounterparts, mainly due to their fast switching and non-volatility.

To better understand the difference between both the biological and the synthetic systems a closer look on neural and synaptic processes is required. Processing information and generation of intelligent behavior in living organisms is highly distributed across billions of neurons. Each neuron is connected via membrane-separated synaptic junctions to multiple other neurons. Information travels across neurons in the form of action potentials that are generated by the active accumulation and dissipation of ionic charge. When this traveling potential exceeds a specific threshold, a neuron initiates the release of chemical neurotransmitters across one or more synapses to communicate with other neurons. Memory is co-localized with processing in a 3D architecture that interweaves synaptic connections between many neurons. The strength or "weight" of a synaptic communication between neurons relies on the time-dependent concentrations of neurotransmitters, ions and other signaling molecules released from the presynaptic neuron, relative to that absorbed by the postsynaptic neuron located directly across the synaptic cleft. The weight of a synapse is also highly adaptable, where changes in receptor sensitivity can amplify or attenuate signaling between the pre- and postsynaptic neurons. This enables adaptability in neuron-to-neuron communication, called plasticity [15, 16], which allows for memory retention over lifetimes from learning that occurs in seconds. Two types of plasticity behaviors occur at the synaptic level: 1) Short-Term Potentiation (STP), and 2) Long-Term Potentiation (LTP) [17]. STP refers to a transient enhancement in synaptic transmission, that could be, usually, attributed to an increase in vesicle release (neurotransmitters) probability. On the other hand, LTP is a persistent enhancement which is attributed to an increase in Ca^{2+} in the post-synaptic site which leads to increase in the AMPA receptors in the post-synaptic site (i.e. early-phase LTP which lasts a few hours), or, if significant enough, to an increase in the conductance of the AMPA receptors along with the creation of new synapses, via increase in transcription factors resulting in gene expression and synthesis of new proteins (i.e. late-phase LTP which lasts from 24 hours up to a lifetime). Another type of synaptic enhancement is paired-pulse facilitation (PPF) which occurs only in the presynaptic terminal. PPF is a form of short-term plasticity which is caused by two presynaptic spikes that are evoked in close succession. Therefore, the dynamics of Ca^{2+} influx and extrusion in the pre- and post-synaptic sites play intricate roles in initiating plasticity in biological synapse, and electronic emulators remain nowhere near close to replicating these dynamics. In a recent study [18] a Ag-in-oxide memristor with a temporal response similar to the of that of the synaptic Ca^{2+} dynamics, was presented. While the proposed memristor represents a major leap toward more biomimetic synaptic dynamics, it is still solid-based and consumes energy levels orders of magnitudes larger than what is required in its biological counterparts.

To address all the aforementioned limitations and uncover new insights into the role of tunable ion transport and synapse-neuron organization on complex computation in the brain, we

present herein a new class of adaptable neuromorphic circuits comprised of biomimetic membranes with reconfigurable ion transport properties that mimic the variable weighing found in real synapses. We demonstrate that the droplet interface bilayer (DIB) is a platform that could serve as a synaptic mimic. DIBs have been successfully used to generate relatively stable bilayers convenient for single-channel electrophysiology and optical imaging from a wide variety of preparations, ranging from purified proteins to reconstituted eukaryotic cell membrane fragments [19, 20]. They have also been used as building scaffolds for stimuli-responsive material systems with a diverse range of applications, such as drug delivery, tissue engineering, biosensors, as well as the detection of biological warfare agents. In its simplest form a DIB consists a synthetic biological membrane formed at the conjoining interface of two lipid-encased aqueous droplets in a bath of oil. The droplets contain voltage-activated alamethicin peptides, capable of creating conductive pathways for ion transport through the impermeable lipid membrane [21]. The insertion of the peptides and formation of transmembrane ion channels is achieved at externally applied potentials higher than ~70 mV. We also discuss an analytical model that describes that electrical behavior of the conductive pathways created by the alamethicin peptides within the highly insulating lipid-membrane. We demonstrate that our system is a "generic" memristor by generating current-voltage planes which exhibit "pinched" hysteretic responses. Moreover, we demonstrate the system's capability of exhibiting STP/PPF behaviors in response to high-frequency 50 ms, 150 mV voltage pulses.

EXPERIMENTAL METHODS

1. Materials

The aqueous phase which form the droplets consist of a suspension of phospholipids vesicles and a buffering agent in highly pure deionized water, while the oil phase consists of Hexadecane (99%, Sigma). The lipid vesicle solution is prepared and stored as described in various previously published articles [22]. The lipids solution contains 2 mg/ml solution of 1,2-diphytanoyl-sn-glycero-3-phosphocholine (DPHPC, Avanti Polar Lipids, Inc.) vesicles in 500mM potassium chloride (KCl, Sigma), 10mM 3-(N-morpholino)propanesulfonic acid (MOPS, Sigma), pH7. The 2 % (w/v) agarose hydrogel solution is mixed with a 500 mM KCl and 10 mM MOPS, pH 7 electrolyte solution. Alamethicin (A.G. Scientific) peptides stored at 0.1% (w/v) in ethanol (Sigma) are diluted in the DPHPC-lipid vesicle solution to yield a final concentration of 1µM.

2. Experimental setup

DIBs are formed between two aqueous droplets suspended in the oil-filled, transparent PDMS reservoir, as described elsewhere [23]. The droplets are 200 nL in volume and are pipetted onto agarose-coated, ball-end silver/silver-chloride (Ag/AgCl) electrodes made of a 150 µm silver wire. The droplets anchor to the gel-coated tips within the oil reservoir. The whole setup is centered on top of an Olympus IX50 inverted microscope. Due to the amphiphilic nature of the DPhPC phospholipids (head is hydrophilic while tails are hydrophobic), a couple minutes after the injection of the aqueous droplets a lipid monolayer is formed at the water-oil interface. By bringing the droplets into contact the oil, at the conjoining interface, is shut out and the lipid-tails from the opposing sides "zip up" to from a highly insulating lipid bilayer membrane. The highly insulating membrane (> 1GΩ) is of 5 to 7 nm in thickness and around 250 µm in diameter. Alamethicin peptides are floating around in the aqueous reservoir, however, they insert and form conductive pathways [24] within the lipid bilayer allowing ions to cross from one side to another following the direction of the flow field.

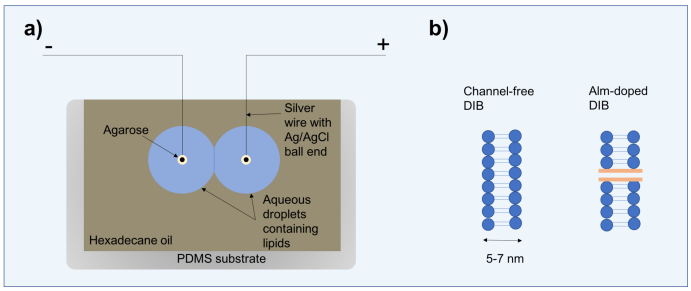

Figure 1. A schematic representing the experimental setup used to characterize DIBs and to study membrane electrophysiology in both channel-free and channel-doped cases. **a)** Aqueous droplets hanging onto two silver wires with chlorided ball ends, which in turn are covered with a thin layer of agarose. The droplets contain both the lipids and the alamethicin peptides. The oil-filled substrate is made of PDMS and placed atop an inverted microscope. The silver wire on the right is connected to the Axopatch 200B headstage (positive lead), while the wire on the left is connected to the ground. **b)** A lipid bilayer forms at the conjoining interface of both droplets. In the case where alamethicin is present in the aqueous phase, a conductive pathway (or multiple) is formed as a results of peptides insertion in response to an externally applied transmembrane potential greater that 70 mV.

3. Electrical measurements

Lipid bilayer interface formed within the biomolecular unit cell is characterized through two types of electrical measurements. Electrically, the lipid bilayer interface is modelled as a capacitor and a resistor in parallel. Therefore, capacitance measurements are carried out in order to verify the increase in capacitance resulting from the bilayer formation. Axopatch 200B and Digidata 1440A (Molecular Devices) are used to measure the resulting square-wave current produced by an external, 10 mV triangular voltage waveform at 10 Hz (Hewlett Packard 3314A function generator). The second type of electrical recording is cyclic voltammetry, which consists of applying a periodic voltage waveform with variable sweep rates and amplitudes, and recording the current response resulting from the membrane or the ion channels. In this article, we use a triangular waveform of variables sweep rates (explained in the RESULTS section) and an amplitude of 190 mV. The current is plotted versus the voltage without any processing.

ANALYTICAL MODELS

1. Macroscopic current-voltage relations for alamethicin ion channels

The current response induced by alamethicin in response to an increase in transmembrane voltage is well characterized [25, 26]. It is, also, well established that the number of pores N is proportional to the current (i.e. the channel conductance), and thus the time course of N may be represented by

$$\frac{dN}{dt} = n - mN, \tag{1}$$

where n and m are the rates of pore formation and decay, respectively. If we define the relation time (τ) to be equal to ($1/m$) and the steady-state number of pores (N_s) to be equal to ($n/m = n\tau$), then equation (1) may be rewritten as

$$\frac{dN}{dt} = \frac{1}{\tau}(N_s - N). \tag{2}$$

The steady-state number of pores is expressed empirically by an exponential function of the applied voltage V [24],

$$N_s = N_0 e^{\left(\frac{V}{V_e}\right)}, \tag{3}$$

where V_e and N_0 are the voltage change required to cause an e-fold increase in the number of pores and the proportionality constant, respectively. The relaxation time τ may also be empirically expressed as an exponential function of the voltage V,

$$\tau = \tau_0 e^{\left(\frac{V}{V_\tau}\right)}, \tag{4}$$

where V_τ and τ_0 are the voltage change required to cause an e-fold increase in τ, the proportionality constant, respectively. From here, we can proceed to develop the relationship conductance-voltage relationship as a function of the sweep rate V_r (previously defined in section 3 in the EXPERIMENTAL METHODS section), as follows

$$\frac{dG}{dV} = G_u \frac{dN}{dV} = G_u \frac{N_0 e^{\left(\frac{V}{V_e}\right)} - N}{V_r \tau_0 e^{\left(\frac{V}{V_\tau}\right)}}, \tag{5}$$

where G_u is the mean unit conductance.

2. Alamethicin ion channels are generic memristors

Figure 2a shows classic electrical models of the lipid bilayer membrane in both the channel-free and Alm-doped cases. The modified G_{Alm} symbol denotes a time-varying alamethicin conductance. The classical way that scientists used to identify the nature of this circuit element (i.e. alamethicin) was by assuming it behaves like a resistor obeying Ohm's law, but whose resistance change with time. We believe that representing alamethicin as a time-varying resistor is an extreme simplification, especially that the steady-state number of pores N_s is an exponential function of the voltage V (i.e. the current-voltage relationship in exponential, not linear as Ohm's law suggests). Therefore, representing the alamethicin ion channels as memristors would be a much more accurate representation (Figure 2b). Given equations (1-5) one may express the conductance of alamethicin ion-channels G_{alm} as a function of the number of pores N, and thus the current-voltage relationship becomes

$$I_{alm} = G_{alm}(N)V_{alm} \tag{6}$$

while,

$$\frac{dN}{dt} = f(N, V_{alm}) = \frac{1}{\tau_0 e^{\frac{V_{alm}}{V_\tau}}}\left(N_0 e^{\frac{V_{alm}}{V_e}} - N\right) \tag{7}$$

The alamethicin ion-channel memristor defined in Figure 2a is therefore an example of a generic memristor described by one state equation (as shown in equations (6) and (7)). (Note: for more information about the analytical characterization of memristors the reader may refer to [5]).

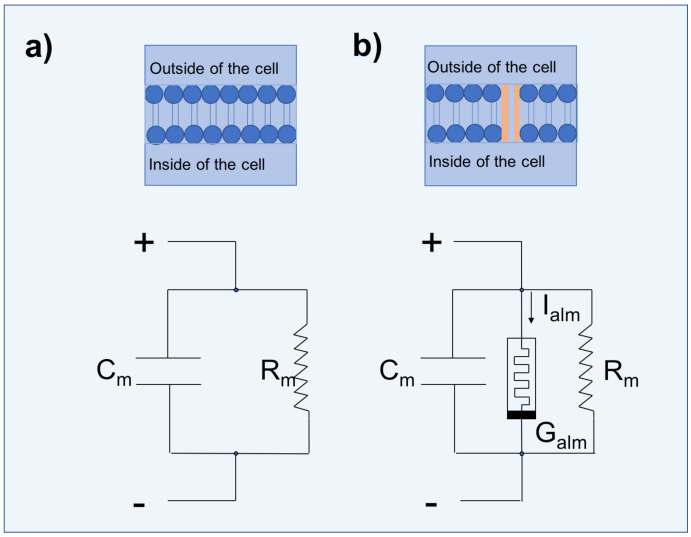

Figure 2. Schematics showing the lipid bilayer membrane in both channel-free and Alm-doped conditions along with their corresponding, equivalent circuits. **a)** A channel-free membrane is electrically defined as a capacitor and a resistor in parallel. The resistance of the membrane is on the Giga-ohm level, due to the insulating nature of the hydrophobic core. **b)** When the alamethicin peptides are introduced and conductive pathways are formed, the channel-free equivalent circuit is modified by introducing a memristor with a conductance G_{alm}. This memristor represent the alamethicin ion channel.

RESULTS AND DISCUSSION

For any device to be characterized as a memristor, 1) it must exhibit a "pinched" hysteresis loop in the voltage-current plane for any bipolar periodic signal excitation, 2) the "pinched"

hysteresis lobe area should decrease monotonically as the excitation frequency increases, and 3) it should shrink to a single-valued function when the frequency tends to infinity. In the previous section, we explained by developing an analytical model why we strongly believe that our system is a generic memristor. In this section, we will experimentally demonstrate how our system satisfies the three conditions mentioned earlier.

1. Pinched hysteresis loops

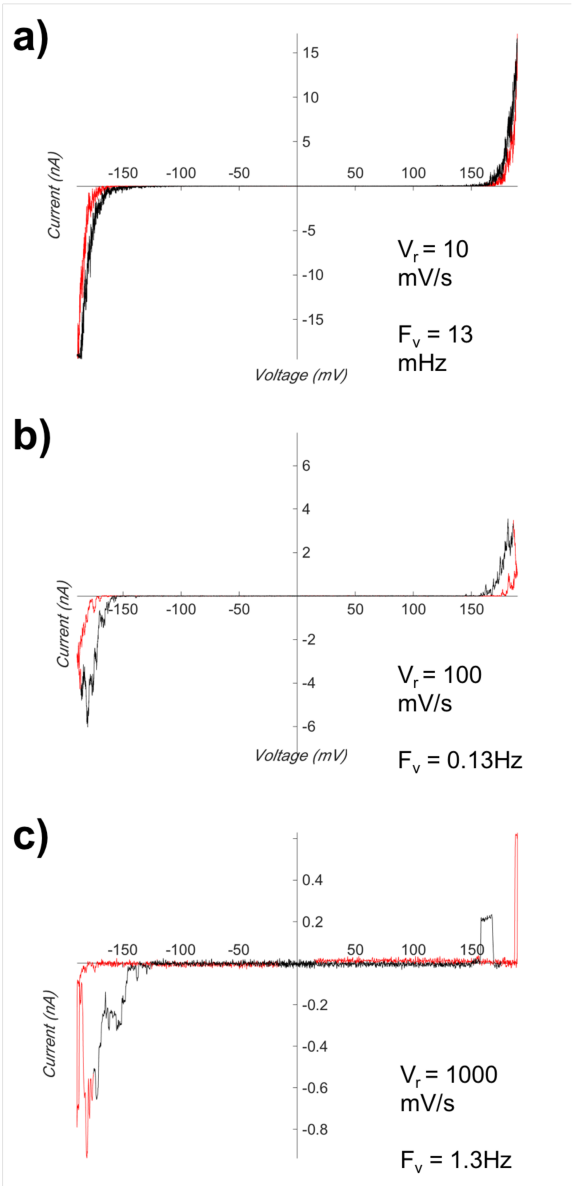

Figure 3. The I-V planes for alamethicin obtained via cyclic voltammetry at three different voltage sweep rates, **a)** 10 mV/s, **b)** 100 mV/s, and **c)** 1000 mV/s. Alamethicin exhibited a "pinched" hysteretic behavior. The red color indicates the current response to an increasing voltage (both in the positive and negative sweeps), while the black color indicates the current response to a decreasing voltage.

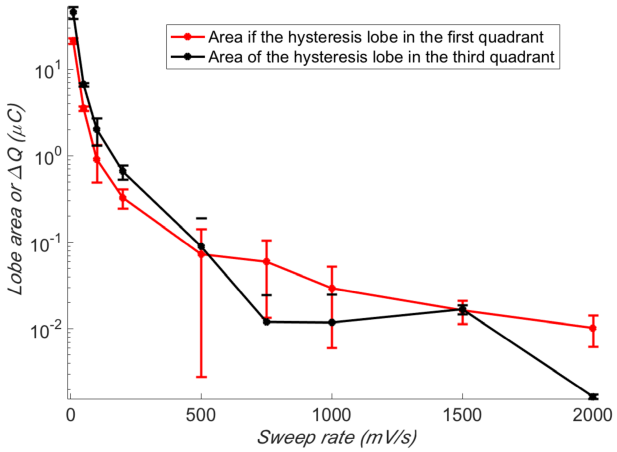

Figure 4. Areas of the hysteresis lobes as a function of voltage sweep rate.

Figure 3 shows the current versus voltage planes (I-V) of alamethicin at three different sweep rates (V_r). The curves are generated via cyclic voltammetry as described in section 3 from the EXPERIMENTAL METHODS section. As expected the I-V curves, in the all cases exhibited a "figure 8" or "pinched" hysteresis response. It also noticeable that the hysteresis widens as the sweep rate increases as shown in figure 3. This is a well-known phenomenon [24], where the hysteresis is believed to be directly related to the channel formation kinetics of alamethicin. Therefore, a slower voltage sweep rate (figure 3a) results in much narrower hysteresis, since the alamethicin has enough time to insert and decay. On the other hand, at higher sweep rates (figures 3b and 3c) the hysteresis is wider. This suggests that hysteresis loop is directly dependent on the voltage sweep rate of the voltage [24]. This relation is described by equation 5, where the rate change in conductance with respect to the voltage is inversely proportional to the voltage sweep rate. So far, the results validate that alamethicin satisfies the first condition to be a memristor.

Next, the areas of the hysteresis lobes in both the first and third quadrants at various voltage sweep rates are computed. Figure 4 shows that as the sweep rate is increased the area of the hysteresis lobe decreases. This satisfies the second condition and further validates that alamethicin is indeed a generic memristor. The maximum sweep rate that we were able to use was 2000 mV/s due to equipment limitations. However, we believe that as the sweep rate tends to infinity the hysteresis would be narrowed into a single-function value equivalent to the electrolyte resistance. We believe that this would be the case since alamethicin would not be able to insert in the membrane, and therefore, the impedance of the membrane reduces to become equal to the that of the electrolyte solution described in section 1 in the EXPERIMENTAL METHODS section.

2. STP and PPF behaviors in response to high frequency voltage pulses

As mentioned in the INTRODUCTION section, a biomimetic, biomolecular memristor is expected to exhibit short-term plasticity, where the application of voltage pulses to synapses may prompt an increase or decrease in postsynaptic responses, as a function of the pulse frequency. In this section, we experimentally demonstrate STP and PPF behaviors with the alamethicin-based memristor. We show, in figure 5, the current response of the alamethicin-doped DIB to voltages pulses (150 mV, 50 ms). The pulse width and duration between pulses are denoted *W* and *T*, respectively. Figure 5 shows that when the time interval between consecutive pulses (*T*) is short (high frequency), alamethicin conductance increases (Figure 5c) from its initial conductance as the number of pulses increases. In contrast, as *T* is longer the conductance of alamethicin drops to zero (i.e. the membrane capacitive current) as no pores are formed (figure 5a). At *T* equal to 25 ms the conductance of alamethicin increases to a value equal to a single-channel conductance before it drops back to zero when the voltage is dropped to zero. This is a typical example of STP behavior where the pores never exhibit a cumulative increase in conductance but rather a repetitive and consistent increase in conductance equivalent to a single-channel insertion. The results show that at *T* equal to 1000 ms no gating of alamethicin is recorded (i.e. weight of the memristor is unchanged and is equivalent to that of a channel-free membrane). It is worth mentioning that while the concentration of alamethicin used in these experiments (1 μM) should yield macroscopic currents at DC potentials (i.e. frequency is equal to zero), we record single-channel currents at each pulse due to the rate of insertion and decay of alamethicin pores in the membrane. At very low frequency (*T*=1000 ms) the pulse duration is faster than the insertion rate of the channels, and thus no pores are inserted leading to no weight change. In contrast, at very high frequency (*T* = 0.5 ms) the pores slowly insert and remain to do so until reaching steady-state. This behavior is comparable to a large extent to LTP in bio-synapses, where high frequency pulses lead to continuous and enhanced release of neurotransmitters leading to a continuous flow of K^+ ions into the post-synapse, which would lead to changes in synapse weight and both early- and late-phase LTP. For better interpretation of the results, we compute the current RMS values at each pulse for three different pulse duration values (Figure 7). At high frequency (black line)

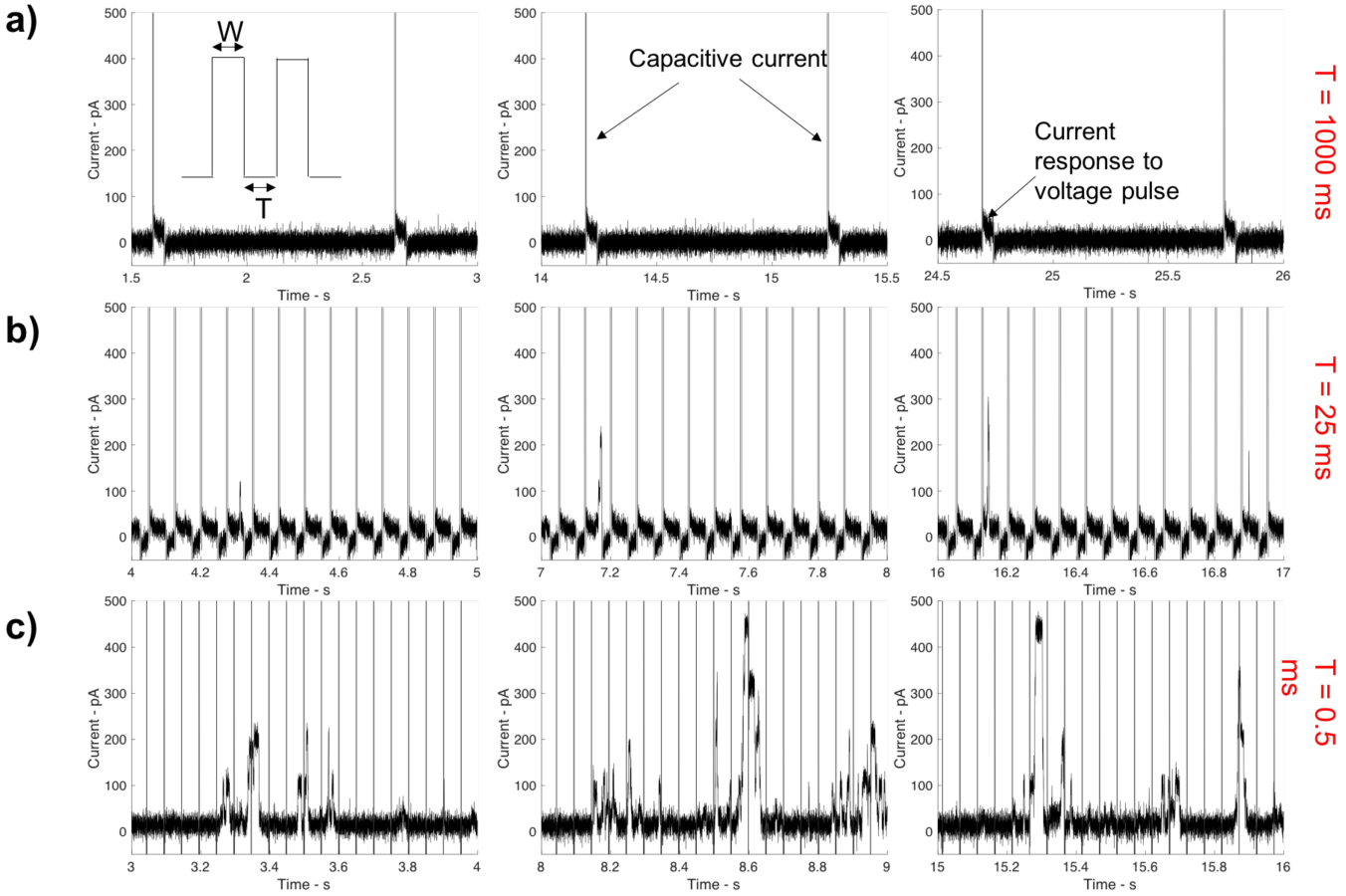

Figure 5. Current response of the alamethicin-dope DIB system to voltage pulses (150 mV, 50 ms). The pulse width (*W*) is chosen to be 50 ms while the amplitude is equal to 150 mV. As shown, the duration between pulses (*T*) is varied between, **a)** 1000 ms, **b)** 25 ms, and **c)** 0.5 ms. The black vertical and parallel lines in all plots are capacitive current spikes resulting from the abrupt increase or decrease in voltage.

the results show that both the RMS currents and the probability of gating increase. The increase in RMS current is defined by the increase in the amplitudes of the sharp spikes with time. In contrast, at low frequency the RMS values are equal and correspond to the membrane capacitance and the noise level. At T equal to 25 ms the small current RMS spikes are repetitive and relatively equal in amplitude. They also occur at a low probability and randomly which is dictated by the stochastic nature of alamethicin.

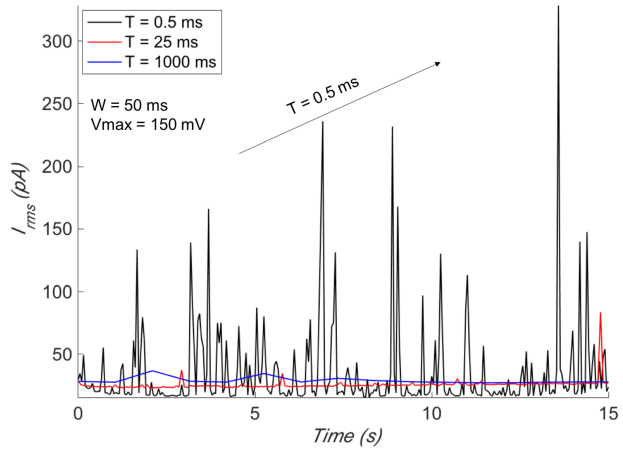

Figure 6. RMS current values at each pulse for three different pulse durations. At low frequency (T = 1000 ms) (blue line) the displayed equal RMS values correspond to the membrane capacitance. The red line corresponds to T = 25 ms, while the black line corresponds to T = 0.5 ms (high-frequency). The RMS values at high frequency increased with time along with the probability of gating - another proof of PPF.

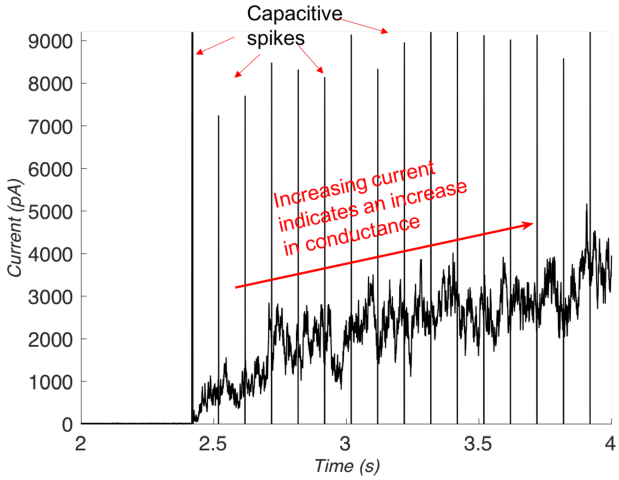

Figure 6. Experimental demonstration of PPF behavior. Current response to multiple subsequent voltage pulses (175 mV, W = 50 ms, T = 1ms). The results show an increase in current (i.e. increase in conductance) demonstrating PPF.

Figure 7 displays the current response of our system to a high-frequency pulse with amplitude of 175 mV (higher than the previous case). The results show that the current increased with time which demonstrates a PPF behavior.

CONCLUSION

We presented herein a new class of adaptable neuromorphic circuits comprised of biomimetic membranes with reconfigurable ion transport properties that mimic the variable weighing found in real synapses. We demonstrated that the droplet interface bilayer (DIB) is a platform that could serve as a synaptic mimic, when alamethicin peptides are inserted and formed conductive pathways. We also discussed an analytical model that describes that electrical behavior of the alamethicin channels within the highly insulating lipid-membrane. The model describes how the conductance of alamethicin is a function of the number of pores in the membrane. The single state-equation model suggests that alamethicin is a generic memristor. Further, we experimentally demonstrated the generic memristive nature of alamethicin by generating current-voltage planes which exhibit “pinched” hysteretic responses. Moreover, we demonstrated the system’s capability of exhibiting STP and PPF behaviors in response to high-frequency 50 ms, 150 mV voltage pulses. An alamethicin-based memristor may represent a revolution in the neuromorphic computing field, as it comes extremely close to mimicking the biological process on both the mechanism and ion transport levels.

ACKNOWLEDGMENTS

We would like to acknowledge the financial support provided by the National Science Foundation Grant NSF ECCS-1631472.

REFERENCES

[1] Mead, C., 1990, "Neuromorphic electronic systems," Proceedings of the IEEE, 78(10), pp. 1629-1636.
[2] Liu, S.-C., 2000, "A neuromorphic aVLSI model of global motion processing in the fly," IEEE Transactions on circuits and systems II: analog and digital signal processing, 47(12), pp. 1458-1467.
[3] Jo, S. H., Chang, T., Ebong, I., Bhadviya, B. B., Mazumder, P., and Lu, W., 2010, "Nanoscale memristor device as synapse in neuromorphic systems," Nano letters, 10(4), pp. 1297-1301.
[4] Diorio, C., Hasler, P., Minch, A., and Mead, C. A., 1996, "A single-transistor silicon synapse," IEEE transactions on Electron Devices, 43(11), pp. 1972-1980.
[5] Chua, L., 2014, "If it’s pinched it’sa memristor," Semiconductor Science and Technology, 29(10), p. 104001.
[6] Chua, L., 2014, "Resistance switching memories are memristors," Memristor Networks, Springer, pp. 21-51.
[7] Chua, L., 1971, "Memristor-the missing circuit element," IEEE Transactions on circuit theory, 18(5), pp. 507-519.
[8] Hickmott, T., 1962, "Low-frequency negative resistance in thin anodic oxide films," J Appl Phys, 33(9), pp. 2669-2682.
[9] Argall, F., 1968, "Switching phenomena in titanium oxide thin films," Solid-State Electronics, 11(5), pp. 535-541.
[10] Strukov, D. B., Snider, G. S., Stewart, D. R., and Williams, R. S., 2008, "The missing memristor found," nature, 453(7191), pp. 80-83.
[11] Yang, J. J., Pickett, M. D., Li, X., Ohlberg, D. A., Stewart, D. R., and Williams, R. S., 2008, "Memristive switching

mechanism for metal/oxide/metal nanodevices," Nat Nanotechnol, 3(7), pp. 429-433.
[12] Kwon, D.-H., Kim, K. M., Jang, J. H., Jeon, J. M., Lee, M. H., Kim, G. H., Li, X.-S., Park, G.-S., Lee, B., and Han, S., 2010, "Atomic structure of conducting nanofilaments in TiO2 resistive switching memory," Nat Nanotechnol, 5(2), pp. 148-153.
[13] Wedig, A., Luebben, M., Cho, D.-Y., Moors, M., Skaja, K., Rana, V., Hasegawa, T., Adepalli, K. K., Yildiz, B., and Waser, R., 2016, "Nanoscale cation motion in TaOx, HfOx and TiOx memristive systems," Nat Nanotechnol, 11(1), pp. 67-74.
[14] Ohno, T., Hasegawa, T., Tsuruoka, T., Terabe, K., Gimzewski, J. K., and Aono, M., 2011, "Short-term plasticity and long-term potentiation mimicked in single inorganic synapses," Nature materials, 10(8), pp. 591-595.
[15] Voglis, G., and Tavernarakis, N., 2006, "The role of synaptic ion channels in synaptic plasticity," EMBO Reports, 7(11), pp. 1104-1110.
[16] Zucker, R. S., and Regehr, W. G., 2002, "Short-Term Synaptic Plasticity," Annual Review of Physiology, 64(1), pp. 355-405.
[17] Bliss, T. V., and Collingridge, G. L., 1993, "A synaptic model of memory: long-term potentiation in the hippocampus," Nature, 361(6407), p. 31.
[18] Wang, Z., Joshi, S., Savel'ev, S. E., Jiang, H., Midya, R., Lin, P., Hu, M., Ge, N., Strachan, J. P., and Li, Z., 2017, "Memristors with diffusive dynamics as synaptic emulators for neuromorphic computing," Nature materials, 16(1), pp. 101-108.
[19] Najem, J. S., Dunlap, M. D., Rowe, I. D., Freeman, E. C., Grant, J. W., Sukharev, S., and Leo, D. J., 2015, "Activation of bacterial channel MscL in mechanically stimulated droplet interface bilayers," Sci Rep, 5, p. 13726.
[20] Sarles, S. A., and Leo, D. J., 2010, "Regulated attachment method for reconstituting lipid bilayers of prescribed size within flexible substrates," Anal Chem, 82(3), pp. 959-966.
[21] Taylor, G. J., Venkatesan, G. A., Collier, C. P., and Sarles, S. A., 2015, "Direct in situ measurement of specific capacitance, monolayer tension, and bilayer tension in a droplet interface bilayer," Soft matter, 11(38), pp. 7592-7605.
[22] Najem, J. S., Dunlap, M. D., Yasmann, A., Freeman, E. C., Grant, J. W., Sukharev, S., and Leo, D. J., 2015, "Multifunctional, Micropipette-based Method for Incorporation And Stimulation of Bacterial Mechanosensitive Ion Channels in Droplet Interface Bilayers," Journal of visualized experiments : JoVE(105).
[23] Taylor, G. J., and Sarles, S. A., 2014, "Heating-enabled formation of droplet interface bilayers using Escherichia coli total lipid extract," Langmuir, 31(1), pp. 325-337.
[24] Okazaki, T., Sakoh, M., Nagaoka, Y., and Asami, K., 2003, "Ion channels of alamethicin dimer N-terminally linked by disulfide bond," Biophysical journal, 85(1), pp. 267-273.
[25] Eisenberg, M., Hall, J. E., and Mead, C., 1973, "The nature of the voltage-dependent conductance induced by alamethicin in black lipid membranes," Journal of Membrane Biology, 14(1), pp. 143-176.
[26] Boheim, G., 1974, "Statistical analysis of alamethicin channels in black lipid membranes," Journal of Membrane Biology, 19(1), pp. 277-303.